Ehleringer, J.R., T.E. Cerling, J.B. West, D.W. Podlesak, L.A. Chesson, and G.J. Bowen. 2008. Spatial considerations of stable isotope analyses in environmental forensics, pages 36-53. In R.E Hester and R.M. Harrison (eds.), Issues in Environmental Science and Technology volume 26. Royal Society of Chemistry Publishing, Cambridge.

ISSUES IN ENVIRONMENTAL SCIENCE AND TECHNOLOGY

EDITORS: R.E. HESTER AND R.M. HARRISON

26
Environmental Forensics

RSC Publishing

Spatial Considerations of Stable Isotope Analyses in Environmental Forensics

JAMES R. EHLERINGER, THURE E. CERLING, JASON B. WEST, DAVID W. PODLESAK, LESLEY A. CHESSON AND GABRIEL J. BOWEN

Stable isotope analyses complement other analytical approaches to chemical identification in an environmental investigation[1] (*e.g.* HPLC, GC–MS, LC–MS), because stable isotope analyses provide an additional 'fingerprint' that further characterizes a piece of forensic evidence. The analysis of stable isotope composition of a material at natural abundance levels provides a means of relating or distinguishing two pieces of evidence that have exactly the same chemical composition.[2,3] The different kinds of materials, approaches and applications of stable isotope analyses to the forensic sciences have been recently reviewed.[2,4–6] Here we focus on a relatively new and different aspect of applying stable isotopes to forensic sciences: sourcing of evidentiary materials with a geo-spatial perspective.

The study of stable isotopes as an environmental forensic tool is based on the ability of an isotope ratio mass spectrometer to measure very small, naturally occurring differences in the abundances of the heavy (rarer) to light (common) stable isotopes in a material and then to relate that isotope ratio composition to other samples or other evidence (elaborated further below). The specific instrumentation with applications considered in this review is the gas isotope ratio mass spectrometer (IRMS), which analyzes gases with a mass of <70.[7] This limits the applications of the IRMS to analyses of the stable isotope composition of hydrogen (H) as H_2, carbon (C) as CO_2, nitrogen (N) as N_2, oxygen (O) as CO, CO_2 or O_2, chlorine (Cl) as CH_3Cl and/or sulfur (S) as SO_2. Evidence or materials may originate in gaseous, liquid or solid states and the materials analyzed vary from simple to complex with high molecular weights. Whenever the evidence or material to be analyzed is complex, a combustion or pyrolysis reaction is coupled prior to the mass spectrometer to convert the materials into

Issues in Environmental Science and Technology, No. 26
Environmental Forensics
Edited by RE Hester and RM Harrison

one of the mentioned gases. In some applications, compound-specific analyses are conducted (*e.g.* *n*-alkanes contained within oil), whereas in others complex biological tissues (*e.g.* bird feathers, hair) and whole organisms are analyzed. For isotope ratio analyses of heavier elements and elements difficult to maintain in a gaseous state, a thermal ionization mass spectrometer (TIMS) is employed. The reader is encouraged to look at recent reviews where the application of TIMS approaches to forensic and sourcing applications has been considered.[8,9]

In forensic studies, investigators often compare individual samples with each other to evaluate the extent to which the samples have overlapping to identical chemical compositions. Stable isotopes add another dimension to these sample comparisons by providing an additional isotopic fingerprint that allows materials of similar chemical composition to be distinguished or to be related.[2,5] When sufficient specimens of materials of a given type and of known origin have been acquired and examined, this database may be useful in assigning a probable geographic region-of-origin to a material based simply on an accumulation of observations, rather than to a first-principles mechanistic basis. Such databases have been accumulated for controlled substances such as marijuana, heroin and cocaine.[10–14] These approaches have been useful in both providing information regarding possible region-of-origin sources of controlled substances and in eliminating other regions as possible source locations.

A recent example that highlights the need for spatial maps is the analysis of heroin specimens seized from a North Korean freighter.[12] Australian police seized 50 kg of heroin hydrochloride from the freighter and another 75 kg of heroin hydrochloride from the offload site on Australian soil. Authorities believed that it was 'highly likely' that North Korea was dealing in illegal drugs. In this case, seized heroin specimens were analyzed and determined to be of unknown origin and could not be assigned a probable source location by comparison with other observations of known authentics in the Drug Enforcement Administration (DEA) database. While such an approach can be used to identify samples of unknown origin, assuming that the isotopic composition of a biologically based material from a geographic region maintained a similar isotopic composition over time (different production periods), as has been with natural plant systems,[15–17] the approach provides no forward-looking perspective on the sample's origins.

A novel approach to geographical assignment may yield greater information and insight, especially in the case when an incomplete database is available. By using first-principles or other models of stable isotope fractionation in organisms and the spatial modeling capacity of geographic information systems (GIS), spatial maps of predicted stable isotope ratios can be constructed.[4,18,19] Analytical results from a specimen can then be compared with the map predictions and potential source locations can be identified. These advances represent cutting edge applications of stable isotope ratios to forensics that will continue to develop over the coming years. As databases and fundamental understanding of stable isotope ratios grow, so will their capacity to aid in forensic work. Here we review the potential of this approach to some aspects of the sourcing of materials of forensic interest.

1 A Background in Stable Isotopes

1.1 Stable Isotopes – a Primer

Different isotopes of an element are based on the numbers of neutrons within the nucleus. Stable isotopes are those isotopes of an element that do not decay through radioactive processes over time. Most elements consist of more than one stable isotope. For instance, the element carbon (C) exists as two stable isotopes, ^{12}C and ^{13}C, and the element hydrogen (H) exists as two stable isotopes, ^{1}H and ^{2}H (also known as deuterium). Table 1 provides the average stable isotope abundances of the elements analyzed by IRMS investigations.

1.2 Isotope Ratio Composition is Presented in Delta Notation

Stable isotope contents are expressed in 'delta' notation as δ values in parts per thousand (‰), where $\delta‰ = (R_s/R_{Std} - 1) \times 1000‰$ and R_s and R_{Std} are the ratios of the heavy to light isotope (*e.g.* $^{13}C/^{12}C$) in the sample and the standard, respectively. We denote the stable isotope ratios of hydrogen, carbon, nitrogen, oxygen and sulfur in delta notation as δ^2H, $\delta^{13}C$, $\delta^{15}N$, $\delta^{18}O$ and $\delta^{34}S$, respectively.

R values have been carefully measured for internationally recognized standards. The standard used for both H and O is Standard Mean Ocean Water (SMOW), where $(^2H/^1H)_{std}$ is 0.0001558 and $^{18}O/^{16}O$ is 0.0020052. The original SMOW standard is no longer available and has been replaced by a new International Atomic Energy Agency (IAEA) standard, V-SMOW. The international carbon standard is PDB, where $(^{13}C/^{12}C)_{std}$ is 0.0112372 and is based on a belemnite from the Pee Dee Formation. As with SMOW, the original PDB standard is no longer available, but the IAEA provides V-PDB with a similar *R* value. Atmospheric nitrogen is the internationally recognized standard with an *R* value of $(^{15}N/^{14}N)_{std}$ of 0.0036765. Lastly, the internationally recognized standard for sulfur is CDT, the Canyon Diablo Troilite, with a value of $(^{34}S/^{32}S)_{std}$ of 0.0450045. Typically, during most stable isotope analyses, investigators would not use IAEA standards on a routine basis. Instead, laboratories establish secondary reference materials to use each day that are traceable to IAEA standards and that bracket the range of isotope ratio values anticipated for the samples.

Table 1 Abundances of stable isotopes of light elements typically measured with an isotope ratio mass spectrometer.

Element	*Isotope*	*Abundance (%)*
Hydrogen	^{1}H	99.985
	^{2}H	0.015
Carbon	^{12}C	98.89
	^{13}C	1.11
Nitrogen	^{14}N	99.63
	^{15}N	0.37
Oxygen	^{16}O	99.759
	^{17}O	0.037
	^{18}O	0.204
Sulfur	^{32}S	95.00
	^{33}S	0.76
	^{34}S	4.22
	^{36}S	0.014

1.3 Gas Isotope Ratio Mass Spectrometer

The instrumentation with applications considered in this review is the gas isotope ratio mass spectrometer, which analyzes gases with a mass of <70.[1] High-precision measurements of the stable isotope abundance in a known compound or material are made by converting that substance into a gas and introducing the gas into the mass spectrometer for analysis. Combustion or pyrolysis of the sample is usually associated with an elemental analyzer and the gases are separated from each other through a GC interface. At the inlet to the mass spectrometer, the purified gas is ionized and the ion beam is then focused and accelerated down a flight tube where the path of the ion species is deflected by a magnet. Based on the different isotopic compositions of the ions, they are differentially deflected by the magnet. For instance, for measurements of the carbon isotope composition of a material, the carbon is oxidized to produce CO_2 and the primary species formed are $^{12}C^{16}O^{16}O$ (mass 44), $^{13}C^{16}O^{16}O$ (mass 45) and $^{12}C^{18}O^{16}O$ (mass 46). In contrast to a traditional mass spectrometer where the strength of the magnet is varied and the ionic species are measured by a single detector, in the isotope ratio mass spectrometer the magnet field is fixed and the different isotopic ionic species are deflected into separate detector cups at the end of the flight tube, allowing for greater sensitivity in the measurement of the $^{13}C/^{12}C$ ratio. Whereas a traditional mass spectrometer may be able to detect a 0.5% difference in the R_s value of $^{13}C/^{12}C$ in a sample such as might occur in ^{13}C-enriched biochemical studies, an isotope ratio mass spectrometer has the capacity to resolve a 0.0002% difference in the R_s value at the low end of the naturally occurring $^{13}C/^{12}C$ range. In the case of CO_2, this is because R_s is measured in an isotope ratio mass spectrometer as the ratio of the simultaneous currents in the two cups: $^{12}C^{16}O^{16}O$ (mass 44) and $^{13}C^{16}O^{16}O$ (mass 45) detectors.

An elemental analyzer, or gas chromatograph, is often coupled to the front end of the isotope ratio mass spectrometer. With such an arrangement, it is then possible to oxidize the sample for C, N or S isotope analyses using the elemental analyzer, separate the different combustion gases using a gas chromatograph and analyze the sample gases as they pass into the inlet of the isotope ratio mass spectrometer (so-called continuous-flow IRMS). In this case, helium is used as a carrier gas, transporting the combustion gas products from the elemental analyzer to the mass spectrometer. Similarly, it is possible to pyrolyze the sample in the elemental analyzer for hydrogen and oxygen isotope ratio analyses. In addition, samples can also be isolated, purified and combusted offline and then introduced into the mass spectrometer for stable isotope analyses. Reference materials of known isotopic composition are analyzed before or after the sample

is analyzed. This improves the accuracy of a measurement by directly comparing the isotope signals of the sample and the working reference materials with each other. As a consequence, a daily calibration is not used with the instrument because essentially every sample is compared with a standard treated to the same preparation and analysis conditions. These working reference materials are identified by the stable isotope community and are exchanged among different laboratories in order to determine the best estimate of the actual stable isotope composition of the working standard. Under the best conditions, there will be many working reference materials reflecting a range of stable isotope ratios and a range of material types (*e.g.* water, plant material, animal tissue).

2 The Stable Isotopes of Water

Most of the water actively involved in today's water cycle is in the oceans, which have globally averaged δ^2H and δ^{18}O values near 0‰ each on the International SMOW scale. As surface ocean waters evaporate into the atmosphere, the clouds formed are isotopically depleted in ^{2}H and ^{18}O relative to the ocean, resulting in an air mass that is isotopically depleted relative to the ocean.[20] In turn, as moisture is condensed from clouds during precipitation events, that water is isotopically enriched in ^{2}H and ^{18}O relative to the cloud, leaving the residual cloud mass isotopically depleted in ^{2}H and ^{18}O relative to the original cloud mass. The process of differential isotope depletion during precipitation results in a predictable pattern of depleted isotope ratios of precipitation as cloud masses move inland.[20] Since the hydrogen and oxygen in precipitation become the primary source of H and O atoms incorporated into carbohydrates, proteins and lipids during microbe, plant and animal growth, these H and O isotopes have the potential to carry a geographically based piece of information that proves to be useful in forensic studies.

2.1 *The Meteoric Water Line*

The predictable relationship between the δ^2H and δ^{18}O values of precipitation is known as the meteoric water line (MWL) and has a globally averaged δ^2H/δ^{18}O slope of approximately 8 and an intercept of +10‰.[20] Precipitation falling near coastal regions on every continent has δ^2H and δ^{18}O values slightly less than 0‰. Successive precipitation events associated with rain out of the residual cloud mass result in precipitation with δ^2H and δ^{18}O values near –200 and –24‰ on the continental interiors, respectively. The δ^2H/δ^{18}O slope of precipitation is temperature sensitive, but for temperate and tropical regions of the world the slope remains near 8.

2.2 *Isotopes of Water on a Spatial Scale*

Over half a century ago, the International Atomic Energy Agency (IAEA) in Vienna established a global network of precipitation sites where the δ^2H and δ^{18}O values of precipitation were monitored on a monthly basis.[21,22] From

these and other observations, both temporal and spatial patterns emerged that established the basis for a global representation of the distribution of isotopes in water on a global basis.

Bowen and colleagues have been able to extrapolate from the available location-specific data of stable isotopes in water to spatial maps of the predicted isotopic composition of water throughout the world.[4,23–25] Analyses of the spatial distributions of hydrogen isotopes of waters across North America and Europe reveal substantial variations in stable isotope ratios (Figure 1), making it possible to distinguish precipitation in many geographical locations on the basis of their δ^2H and δ^{18}O values. There are no unique stable isotope ratio values for waters in a specific geographic location, but rather gradients or bands of different isotope ratio values allowing one to distinguish between locations if they were sufficiently far apart from each other. Today it is possible to estimate reliably the globally averaged δ^2H and δ^{18}O values of precipitation for different latitudes and longitudes using a calculator available at http://waterisotopes.org. The spatial integration of these calculations is the map shown in Figure 1. This map of incoming precipitation values is appropriate for use in addressing the stable isotope variations of plants, animals and microbes across the landscape that use this water source during their growth. A second and slightly different water map is generated when tap waters are measured.[19,26] Such a map differs because of water transportation and storage issues, each of

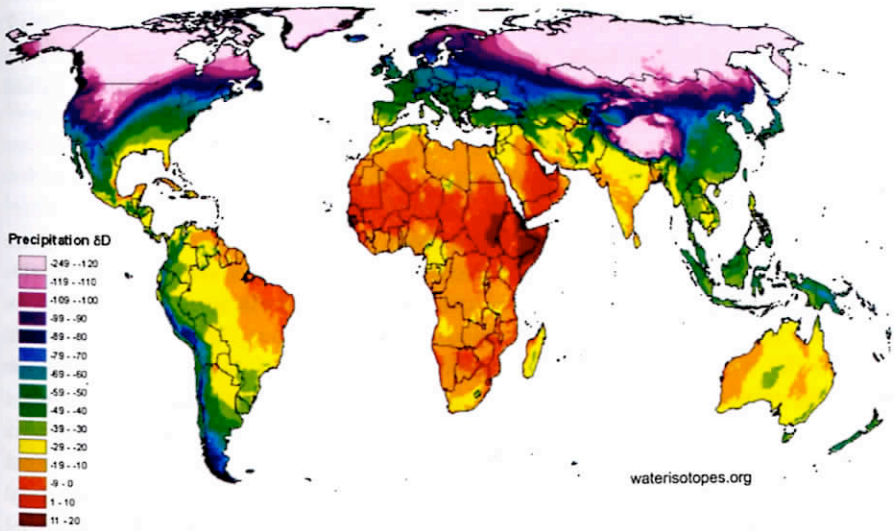

Figure 1 Predicted long-term annual average precipitation hydrogen isotope ratios for the land surface. This continuous layer is produced with a combination of empirical relationships between measured precipitation δ^2H and latitude and elevation and a geostatistical smoothing algorithm for variations not explained by that relationship. Measured precipitation values are those maintained in the IAEA water isotope database. Methods and grids are available at http://waterisotopes.org.

which can result in δ^2H and δ^{18}O values that are similar to the values expected from incoming precipitation or somewhat more enriched or depleted.

3 Spatial Forensic Applications Based on H and O Isotopes

Natural isotope fractionation processes and fractionation steps associated with the synthesis of biological products lead to a wide range of stable isotope ratio values in plants, animals and microbes.[27–31,3] Since these biological materials are based on the isotopic composition of water as a substrate, to a first approximation we anticipate a strong correlation between the isotope ratios of precipitation in a region and those of organisms living in that region. However, the actual δ^2H and δ^{18}O values of the carbohydrates, proteins and lipids in biological organisms will differ from those of their water source because of fractionation events associated with the physical environment and fractionation processes during biosynthesis.

In this section, we consider three classes of biologically derived materials that might be analyzed in a forensic case: plant products used in manufacturing, food products and animal systems. For each, we consider relationships between the isotope ratio of precipitation as a measure of geographic location and the fractionation events, which become permanently recorded in the organic matter of biological tissues. Each approach is built on the relationships among the stable isotope ratio of water at a location, statistically derived climatic conditions at that location and the mechanistic relationships relating fractionation events between substrate and product. Since there is often a wide range of δ^2H and δ^{18}O values in biological materials, this provides an opportunity both to predict and to detect stable isotope ratio differences among samples of forensic, anthropological, ecological and economic interest.

3.1 Cotton as an Example of Plant Sourcing

Plant fibers are of fundamental importance to all of us today, appearing in countless products used on a daily basis. Some of these widespread fiber applications include paper, packaging, construction and clothing. Consider cotton, one of the most important fiber-producing plants and widely grown around the world (Figure 2). Identifying the origins of cotton fibers poses a challenge to the forensic scientist interested in, for example, tracing the origins of a document printed on paper containing cotton fibers or to commercial parties interested in determining if Egyptian cotton bedding had been produced in Egypt or cultivated elsewhere in the world. Here, isotope ratio analyses may offer insights, because spatial patterns in the isotope ratios of cotton are predictable and distinguishable on global scales.

Cotton fibers are composed of cellulose and the hydrogen and oxygen isotope ratios of cellulose molecules are predictable based on mechanistic models.[31] Cellulose contains hydrogen and oxygen atoms derived from water during plant growth and subsequently influenced by atmospheric conditions and biochemical fractionation processes.[31–35] The same mathematical approach allows predictions

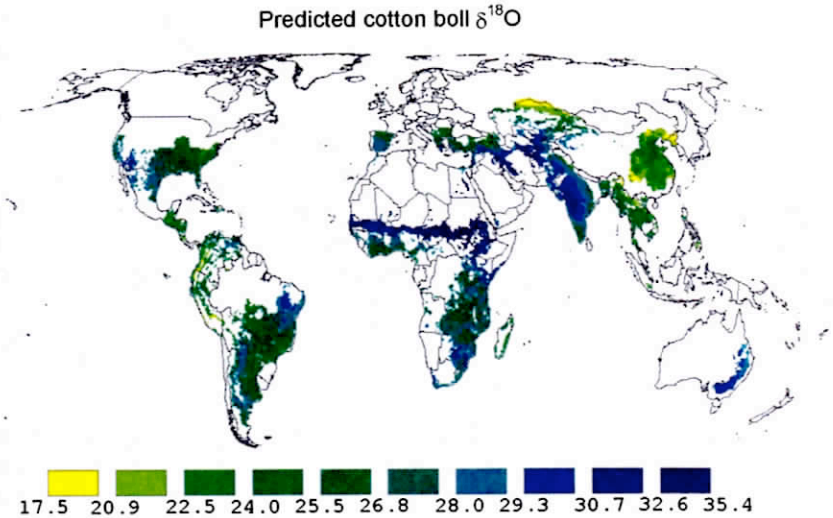

Figure 2 A GIS-based map of the predicted oxygen isotope ratio variations of cellulose in cotton fibers expected on the basis of geographical variations in the isotope ratio of water and of the climatic conditions. Unpublished data from J. Ehleringer and J. West.

of the hydrogen and oxygen isotope ratios of cellulose produced in different plant parts: cotton bolls (a reproductive structure), jute (derived from leaf cellulose) or wood (after extracting cellulose from non-cellulose components).

The models used to predict cellulose isotope ratios in plants are utilized to generate spatial predictions using geographic information system approaches. West *et al.*[36] incorporated the mathematics of cellulose isotope fractionation models for both the organic hydrogen and oxygen atoms contained within cellulose. Combining this mathematical approach with grid-cell estimates of both the stable isotope composition of water and the appropriate climate statistics, it is possible to make predictions of the anticipated hydrogen and oxygen isotope ratios for cellulose produced in different parts of the globe. By overlaying the growth locations of cotton with predicted cellulose isotope values, it is possible to derive a global map of the predicted hydrogen and oxygen isotope ratios of cotton fibers (Figure 2).

One advantage of a global map of the hydrogen or oxygen isotope ratios of cotton fibers is that it allows an application common to forensic science: is the evidentiary material consistent with or not consistent with the value of a sample from a specific region? This allows an investigator either to eliminate a location from further consideration or to use the positive result in a corroborative manner when combined with other supporting information. In few cases will there ever be uniquely predicted hydrogen and oxygen isotope ratios for materials such as cellulose. This is simply because of environmental overlap in homologous climatic regions of the world.

One application is analyses of the geographical origins of high-quality counterfeits of security documents, such as currency. Since the mid-1990s, there

has been an ongoing investigation by the US Secret Service to determine the origins of the 'Supernote', a very high-quality counterfeit $100 bill.[37,38] Reports have suggested that these 'Supernotes' originated from the Middle East through North Korea. One can imagine that isotope ratio analyses of the fibers in these counterfeit currencies might allow three points to be clarified. Are the counterfeit currency specimens consistent with (a) currency paper currently in use by the US government, (b) cotton fibers that are produced in different parts of the Middle East and (c) cotton fibers that are produced in different parts of North Korea? The answers to these questions are of forensic interest in tracing the origins of these high-quality counterfeit notes.

3.2 *Wine as an Example of Food Sourcing*

Hydrogen and oxygen stable isotope ratios have been explored as useful markers of geographic source, production methods and even vintages of wines.[39–42] The methods currently in use require large databases of authentic samples for comparison with suspect samples. Identifying or verifying the geographic source of wine can also be addressed with a complementary approach that is based on model descriptions of the spatial variation in expected wine isotope ratios over a large region. These model descriptions can be developed based on first-principles (*e.g.* the biophysics of isotope fractionation in wine grapes) or on regression or other model-fitting approaches.

The regression approach has been used to model successfully wine oxygen isotope ratio variation using GIS.[43] We extend the spatial extent of this model here for all of Washington, Oregon and California (Figure 3) to demonstrate the potential power of the regression/GIS approach. This GIS-based extrapolation allows one to predict the expected values for regions not yet sampled or values anticipated for a region, were grapes to be grown in that region at some time in the future. The approach also provides a basis for predicting the anticipated isotope ratios of mixtures, where grape juices were derived from different geographical regions.

Some combination of database development and spatial modeling of wine stable isotope ratios will continue to be an important tool as consumer demand for terroir (loosely a sense of place) increases. The use of the database approach has been successful in the European Union and will likely continue to be an important source of verification using stable isotope ratios of wine. Emerging approaches that take advantage of spatial tools such as GIS and improved mechanistic understanding of fractionating processes in grapes and the vinification process will continue to enhance the utility of stable isotopes in geographic sourcing of wine.

3.3 *Keratin as an Example of Animal Sourcing*

Geographic variations in the hydrogen and oxygen isotope ratios of water also form a basis of a geographic signal recorded in the hydrogen and oxygen isotope ratios of organic matter in animals, such as humans,[29,44–46] birds,[47,48] small vertebrates[30,49–51] and microbes.[52,53] Here possible applications related to sources of mad cow disease, vectors associated with bird flu, testing compliance

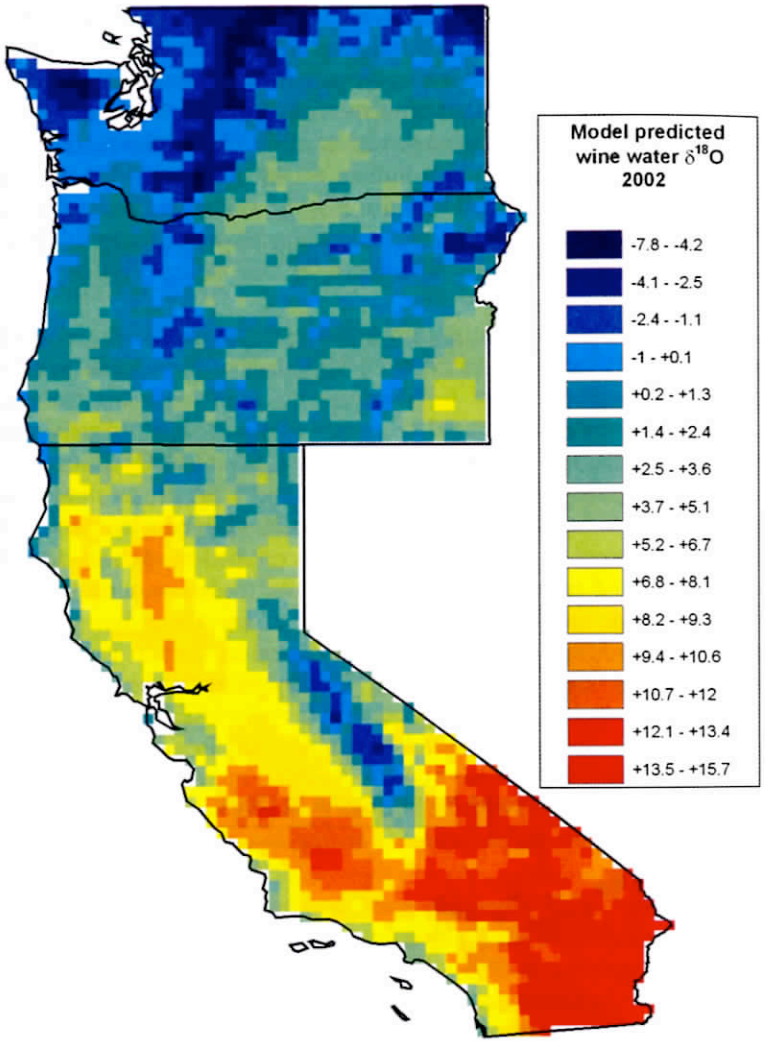

Figure 3 A GIS-based map of the predicted oxygen isotope ratio variations of water in wine expected on the basis of geographical variations in the isotope ratio of source water and of the climatic conditions. Based on information published in West *et al.*[43]

with food production regulations, analyses of CITES-related specimens and verification of region-of-origin claims, especially for high-value products, are all contributing to an increased interest in stable isotope analysis in forensic analyses and food authenticity.[46,54–57]

Hair and fingernails record dietary and water source information and in so doing provide geographic information for forensic studies. Several recent studies have suggested that isotope ratio differences in human hair can be used to distinguish individuals of different geographic origin.[44,46,58,59]

A recent study of public interest involving stable isotopes was the case of the Ice Man discovered on the border between Austria and Italy.[60] Fingernails are also composed of keratin, the same protein as found in hair. Recently, Nardoto *et al.*[61] have shown that citizens from Europe, USA and Brazil can be distinguished based on the isotope ratios within their fingernails. Although there is a tendency among modern human societies for a global supermarket that would homogenize diets and reduce isotope variations among fingernails of different individuals, the diets in these countries are sufficiently distinct so as still to result in detectable differences in the isotope ratios of human fingernails.

As humans and other mammals move through regions that have water with isotopically distinct values, the δ^2H and δ^{18}O values of hair should sequentially record that movement. Figure 4 illustrates this point with the isotope ratio analysis of hair from a horse as that animal was raised in Virginia and then transported to Utah. The abrupt changes in the δ^2H and δ^{18}O values of the hair reflect the transportation of the horse across the USA to its new home. By knowing the growth rate of horse hair, it is possible to reconstruct the temporal patterns of movement. Cerling *et al.*[30] have developed models to describe the multiple dietary and tissue pools that contribute to determining the turnover rate of amino acids feeding into the synthesis of keratin in hair, providing a mechanistic explanation of why the region-to-region shift in isotope ratios is not instantaneous and also providing dietary insights into the fine-scale

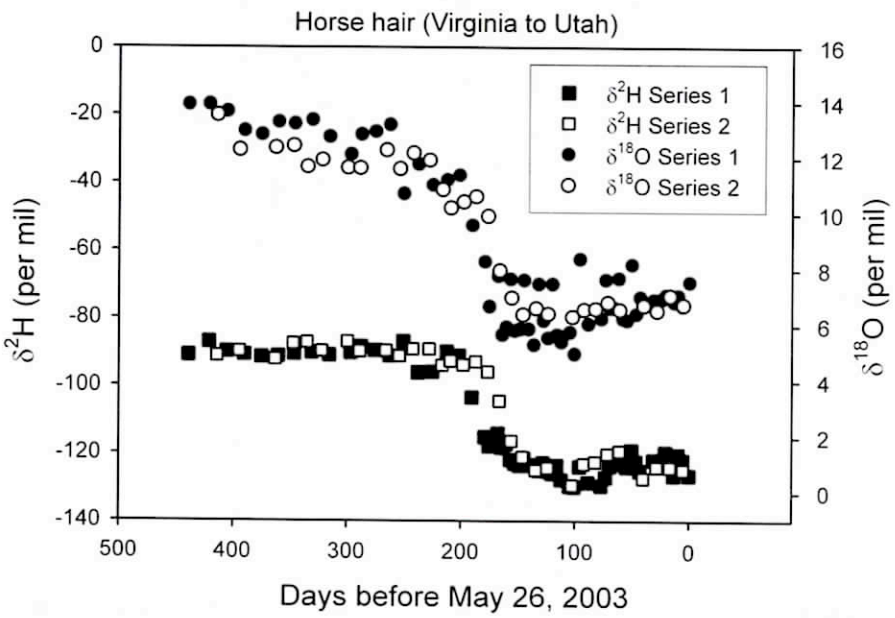

Figure 4 Analysis of the hydrogen and oxygen isotope ratios of sequential tail hair segments from a horse that was moved from Virginia to Utah.

temporal patterns seen in analyses of hair segments. Ehleringer *et al.*[29] have provided a mechanistic model relating the δ^2H and δ^{18}O values of hair, diet and water source. The inversion of such models allows one to use water isotope maps, such as that in Figure 1, to extrapolate to the possible geographic regions that would be consistent with the geographic movements of the horse, were that information not previously known.

4 Opportunities to Examine C and N Isotopes on a Spatial Basis

Plants and animals often exhibit wide ranges in the carbon isotope ratios of their tissues that are related to geographical patterns.[28,46,62–64] For example, the δ^{13}C values of human hair can range from –25 to –10‰, reflecting dietary sources in different parts of the world.[59,65,66] This is because carbon isotope ratios in food can also range from –30 to –10‰, depending on the plant's photosynthetic pathway.[28,62,63,67] One challenge is to place carbon isotope ratio variations into a geographical context that is as established in theory as it is for hydrogen and oxygen isotopes described in previous sections.

4.1 The Imprint of Photosynthetic Pathways

Plants can be divided into two primary photosynthetic pathway groups: C_3 and C_4 photosynthesis.[28] These two pathways exhibit distinctive differences in their δ^{13}C values, with C_3 plants tending to have carbon isotope ratios of about –27‰ and C_4 plants about –12‰.[28] Among the foods we eat, most tend to be C_3 plants, including most grains, fruits and starchy foods. In contrast, the most common C_4 plants are warm-season grasses, which include corn, sorghum, millet and sugarcane.

Figure 5 illustrates the large and non-overlapping differences in the carbon isotope ratios of C_3 plants, ranging from –30 to –24‰ (*e.g.* wheat, barley, potatoes), and C_4 plants, ranging from –14 to –10‰ (*e.g.* corn, millet, sorghum, sugarcane).[28] It is well established that the isotope ratios of assimilated dietary inputs are subsequently recorded in the proteins, lipids, carbonates and carbohydrates of the muscle, bones, teeth and hair of organisms, providing a record of the diet of that organism.[50,68–76] There are consistent 1–3‰ offsets in the carbon isotope ratios of animal tissues relative to the food substrate that was eaten. Isotopic turnover rates are not constant among body tissues, resulting in the tissue-specific integration of dietary inputs over different temporal periods. Turnover rates of carbon isotopes in blood are on the order of days, whereas turnover rates of bone collagen can be on the order of 4–6 years. Although analyses of these tissues will not yield temporal sequence information related to diet of immediate forensic interest, these measures do provide a longer term record of average dietary inputs. It is only the carbon isotope signal in hair and fingernails that provides a high-resolution temporal record of dietary intake.

Understanding the fine-scale spatial significance of δ^{13}C values remains a challenge in omnivores, such as humans, because whereas plant-based inputs

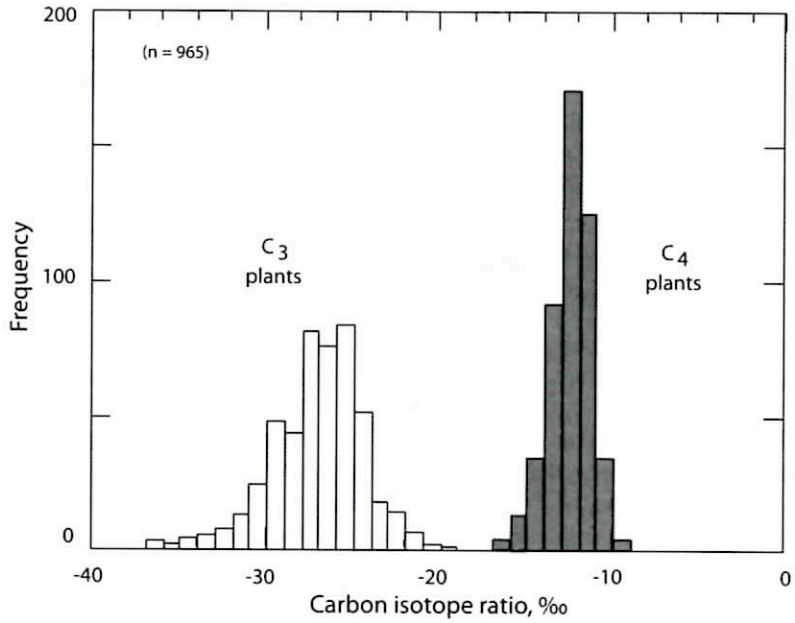

Figure 5 Plants with C_3 versus C_4 photosynthetic pathways have distinct, non-overlapping carbon isotope ratio distributions. Animals that eat C_3 versus C_4 plants will retain an isotopic history of this food source in the hair, bones, teeth and muscle tissues. Based on Cerling *et al.*[63]

might reflect local sources, that is not often the case with animal-based protein sources. For herbivores, the linkages between diet and geography appear to be more closely related. Several models have been developed that incorporate spatial models of variations in the $\delta^{13}C$ values of plant communities on a global scales.[77,78] The Still *et al.*[78] approach categorized communities as C_3 dominated, C_4 dominated or a mixture of both pathways. Given that the distribution of C_4 plants is strongly influenced by temperatures during the growing season, they were able to produce a global $\delta^{13}C$ map based on grid cell temperature values. Subsequently, the Suits *et al.*[77] approach is based on C_3 photosynthesis models with carbon isotope discrimination based on observed meteorology from the European Center for Medium-Range Weather Forecasts. These approaches have not yet been applied to forensic science, but there are distinct possibilities of using such approaches to distinguish geographical origins of border-seized mammals and birds based on $\delta^{13}C$ analyses.

Adulteration of food products through the addition of corn- or sugarcane-based carbon can be easily observed and is frequently detected in USA foods. C_4-derived sugars are frequently used to adulterate the carbohydrates contained in jams, jellies and honeys[2,79] and fermentation sources used in making beer,[80] wines[81] and distilled spirits.[82] However, placing this information on a geographically based approach is not possible, making it challenging to consider the sourcing or the geographical origins of C_4-adulterated food products.

4.2 Cocaine Origins are Reflected in C and N Isotopes

For two decades, there has been international forensic interest in using stable isotope ratio analyses to analyze drugs of abuse, particularly heroin and cocaine.[83–85] Approximately a decade ago, the US DEA launched an effort to obtain sufficient authentic specimens with which to develop a region-of-analysis program. These results were positive. Dual-isotope plots described different spatial realms, providing an approach for distinguishing regions of interest. As part of this collaborative effort, Ehleringer *et al.*[11] showed that the major growing regions of coca for cocaine in South America could be characterized by plots of the carbon versus nitrogen isotope ratios of purified cocaine (Figure 6). In this case, the combination of these two isotopes alone explained more than 80% of the observed variation among samples originating from different growing regions. This information is useful in law enforcement for strategic and intelligence purposes. Today, stable isotope analyses are a key measurement in the DEA's Cocaine Signature Program, providing critical information about the origins of seized samples.

The challenge is to translate the information contained in the carbon and nitrogen isotope ratios of cocaine into a semi-mechanistic model that can be integrated into GIS mapping, as was shown earlier for hydrogen and oxygen isotopes. Because the mixing of carbon dioxide into different layers of the atmosphere is relatively rapid, there are no pronounced spatial gradients in the isotope ratios of atmospheric carbon dioxide, the photosynthetic substrate that forms the basis of all carbon in plants. Instead, there are variations in the fractionation against ^{13}C during photosynthesis.[28] These fractionation events are driven by the degree of stomatal opening,[86–88] leading to regional-to-continental patterns associated with different climate zones.[89–91] Thus, carbon isotope

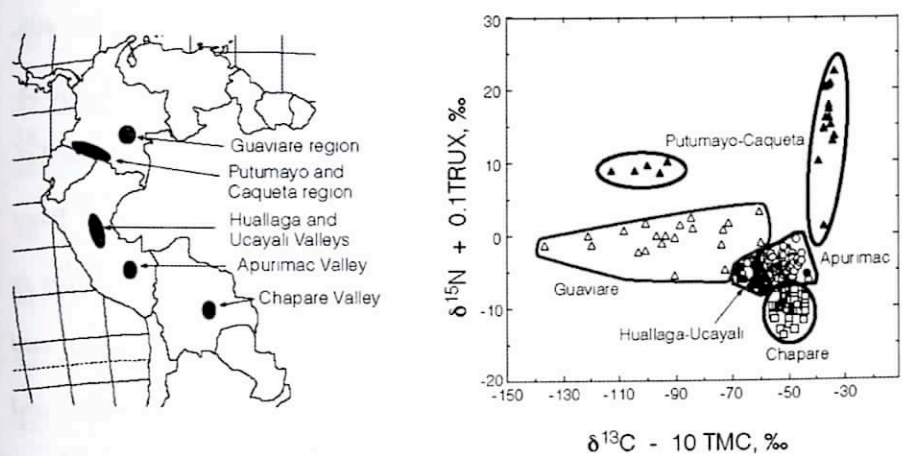

Figure 6 Carbon and nitrogen stable isotope ratios allowed the correct identification of country of origin of 90% of 200+ cocaine samples analyzed (from Bolivia, Colombia or Peru). Based on data in Ehleringer *et al.*[11]

variations among C_3 plants are likely to follow precipitation clines, especially since humidity and precipitation are so closely co-linked across sites. Although the challenge of placing C_3-based ^{13}C variations on to a global scale is challenging, the coherent patterns that appear in the carbon-nitrogen isotope plot of Figure 6 provide support for potential forensic applications once these modeling challenges have been met.

References

1. C. Brunnee, *Rapid Commun. Mass Spectrom.*, 1997, **11**, 694–707.
2. J. R. Ehleringer, T. E. Cerling and J. B. West, in *Forensic Analysis on the Cutting Edge: New Methods for Trace Evidence Analysis*, ed. R. D. Blackledge, Wiley, San Diego, 2007, pp. 399–422.
3. J. B. West, G. J. Bowen, T. E. Cerling and J. R. Ehleringer, *Trends Ecol. Evolut.*, 2006, **21**, 408–414.
4. G. J. Bowen, L. I. Wassenaar and K. A. Hobson, *Oecologia*, 2005, **143**, 337–348.
5. S. Benson, C. Lennard, P. Maynard and C. Roux, *Forensic Sci. Int.*, 2006, **157**, 1–22.
6. W. Meier-Augenstein and R. H. Liu, in *Advances in Forensic Applications of Mass Spectrometry*, ed. J. Yinon, CRC Press, Boca Raton, FL, 2004, pp. 149–180.
7. J. T. Brenna, T. N. Corso, H. J. Tobias and R. J. Caimi, *Mass Spectrom. Rev.*, 1997, **16**, 227–258.
8. K. Pye and D. J. Croft, eds. *Forensic Geoscience: Principles, Techniques and Applications*, Geological Society, London, 2004.
9. B. L. Beard and C. M. Johnson, *J. Forensic Sci.*, 2000, **45**, 1049–1061.
10. J. R. Ehleringer, D. A. Cooper, M. J. Lott and C. S. Cook, *Forensic Sci. Int.*, 1999, **106**, 27–35.
11. J. R. Ehleringer, J. F. Casale, M. J. Lott and V. L. Ford, *Nature*, 2000, **408**, 311–312.
12. J. Casale, E. Casale, M. Collins, D. Morello, S. Cathapermal and S. Panicker, *J. Forensic Sci.*, 2006, **51**, 603–606.
13. E. K. Shibuya, J. E. S. Sarkis, O. Negrini and L. A. Martinelli, *Forensic Sci. Int.*, 2006, **167**, 8–15.
14. T. M. Denton, S. Schmidt, C. Critchley and G. R. Stewart, *Aust. J. Plant Physiol.*, 2001, **28**, 1005–1012.
15. P. W. Rundel, J. R. Ehleringer and K. A. Nagy, eds. *Stable Isotopes in Ecological Research*, Springer, New York, 1988.
16. H. Griffiths, ed. *Stable Isotopes Integration of Biological, Ecological and Geochemical Processes*, BIOS Scientific Publishers, Oxford, 1998.
17. J. R. Ehleringer, A. E. Hall and G. D. Farquhar, eds. *Stable Isotopes and Plant Carbon/Water Relations*, Academic Press, San Diego, 1993.
18. A. Dutton, B. H. Wilkinson, J. M. Welker, G. J. Bowen and K. C. Lohmann, *Hydrol. Process.*, 2005, **19**, 4121–4146.
19. G. Bowen, J. Ehleringer, L. Chesson, E. Stange and T. Cerling, *Water Resour. Res.*, 2007, **43**, W03419.

20. J. R. Gat, *Annu. Rev. Earth Planet. Sci.*, 1996, **24**, 225–262.
21. K. Rozanski, L. Araguas-Araguas and R. Gonfiantini, *Science*, 1992, **258**, 981–985.
22. Y. Yurtsever, *Worldwide Survey of Stable Isotopes in Precipitation*, Report of the Section of Isotope Hydrology, IAEA, Vienna, 1975.
23. G. J. Bowen and J. Revenaugh, *Water Resour. Res* 2003, **39**, 1299.
24. G. J. Bowen and B. Wilkinson, *Geology*, 2002, 30.
25. G. J. Bowen, D. A. Winter, H. J. Spero, R. A. Zierenberg, M. D. Reeder, T. E. Cerling and J. R. Ehleringer, *Rapid Commun. Mass Spectrom.*, 2005, **19**, 3442–3450.
26. G. J. Bowen, T. E. Cerling and J. R. Ehleringer, in *Stable Isotopes as Indicators of Ecological Change*, eds. T. E. Dawson and R. T. W. Siegwolf, Academic Press, San Diego, 2007, pp. 285–300.
27. G. D. Farquhar, J. Lloyd, J. A. Taylor, L. B. Flanagan, J. P. Syvertsen, K. T. Hubick, S. C. Wong and J. R. Ehleringer, *Nature*, 1993, **363**, 439–443.
28. G. D. Farquhar, J. R. Ehleringer and K. T. Hubick, *Annu. Rev. Plant Physiol. Plant Mol. Biol.*, 1989, **40**, 503–537.
29. J. R. Ehleringer, G. J. Bowen, L. A. Chesson, A. G. West, D. Podlesak and T. E. Cerling, *Proc. Natl. Acad. Sci. USA*, in press.
30. T. E. Cerling, L. K. Ayliffe, M. D. Dearing, J. R. Ehleringer, B. H. Passey, D. W. Podlesak, A. M. Torregrossa and A. G. West, *Oecologia*, 2007, **151**, 175–189.
31. J. S. Roden, G. G. Lin and J. R. Ehleringer, *Geochim. Cosmochim. Acta*, 2000, **64**, 21–35.
32. J. S. Roden and J. R. Ehleringer, *Plant Physiol.*, 1999, **120**, 1165–1173.
33. J. S. Roden and J. R. Ehleringer, *Oecologia*, 2000, **123**, 481–489.
34. L. Sternberg and M. J. DeNiro, *Science*, 1983, **220**, 947–949.
35. C. J. Yapp and S. Epstein, *Geochim. Cosmochim. Acta*, 1982, **46**, 955–965.
36. J. B. West, A. Sobek and J. R. Ehleringer, *PLoS Biology*, 2007, in review.
37. I. Silverman, *New Yorker*, October 23, 1995, 50.
38. S. Mihm, *New York Times*, July 23, 2006.
39. N. L. Ingraham and E. A. Caldwell, *J. Geophys. Res.*, 1999, **102**, 2185–2194.
40. I. J. Kosir, M. Kocjaneic, N. Ogrinc and J. Kidric, *Anal. Chim. Acta*, 2001, **429**, 195–206.
41. G. Martin, D. Odiot, V. Godineau and N. Naulet, *Appl. Geochem.*, 1989, **4**, 1–11.
42. G. Martin, C. Guillou, M. L. Martin, M. T. Cabanis, Y. Tep and J. Aerny, *J. Agric. Food Chem.*, 1988, **36**, 316–322.
43. J. B. West, J. R. Ehleringer and T. E. Cerling, *J. Agric. Food Chem.*, 2007, **55**, 7075–7083.
44. I. Fraser, W. Meier-Augenstein and R. M. Kalin, *Rapid Commun. Mass Spectrom.*, 2006, **20**, 1109–1116.
45. D. M. O'Brien and M. J. Wooler, *Rapid Commun. Mass Spectrom.*, 2007, **21**, 2422–2430.

46. Z. D. Sharp, V. Atudorei, H. O. Panarello, J. Fernandez and C. Douthitt, *J. Archaeol. Sci.*, 2003, **30**, 1709–1716.
47. K. A. Hobson and L. I. Wassenaar, *Oecologia*, 1997, **109**, 142–148.
48. C. P. Chamberlain, J. D. Blum, R. T. Holmes, F. Xiahong, T. W. Sherry and G. R. Graves, *Oecologia*, 1997, **109**, 132–141.
49. K. A. Hobson, L. Atwell and L. I. Wassenaar, *Proc. Natl. Acad. Sci. USA*, 1999, **96**, 8003–8006.
50. B. H. Passey, T. F. Robinson, L. K. Ayliffe, T. E. Cerling, M. Sponheimer, M. D. Dearing, B. L. Roeder and J. R. Ehleringer, *J. Archaeol. Sci.*, 2005, **32**, 1459–1470.
51. D. W. Podlesak, A.-M. Torregrossa, J. R. Ehleringer, M. D. Dearing, B. H. Passey and T. E. Cerling, *Geochim. Cosmochim. Acta.*, 2008, **72**, 19–35.
52. H. W. Kreuzer-Martin and K. H. Jarman, *Appl. Environ. Microbiol.*, 2007, **73**, 3896–3908.
53. H. W. Kreuzer-Martin, M. J. Lott, J. Dorigan and J. R. Ehleringer, *Proc. Natl. Acad. Sci. USA*, 2003, **100**, 815–819.
54. M. Boner and H. Forstel, *Anal. Bioanal. Chem.*, 2004, **378**, 301–310.
55. S. Kelly, K. Heaton and J. Hoogewerff, *Trends Food Sci. Technol.*, 2005, **16**, 555–567.
56. A. Rossmann, *Food Rev. Int.*, 2001, **17**, 347–381.
57. L. A. Chesson, A. H. Thompsaon, D. W. Podlesak, T. E. Cerling and J. R. Ehleringer, *Journal of Agricultural and Food Chemistry*, 2007, in review.
58. T. C. O'Connell, R. E. M. Hedges, M. A. Healey and A. H. R. Simpson, *J. Archaeol. Sci.*, 2001, **28**, 1247–1255.
59. T. C. O'Connell and R. E. M. Hedges, *Am. J. Phys. Anthropol.*, 1999, **108**, 409–425.
60. S. A. Macko, G. Lubec, M. Teschler-Nicola, V. Andrusevich and M. H. Engel, *FASEB J.*, 1999, **13**, 559–562.
61. G. Nardoto, S. Silva, C. Kendall, J. Ehleringer, L. Chesson, E. Ferraz, M. Moreira, J. Ometto and L. Martinelli, *Am. J. Phys. Anthropol.*, 2006, **131**, 137–146.
62. J. R. Ehleringer, T. E. Cerling and B. R. Helliker, *Oecologia*, 1997, **112**, 285–299.
63. T. E. Cerling, J. M. Harris, B. J. MacFadden, M. G. Leakey, J. Quade, V. Eisenmann and J. R. Ehleringer, *Nature*, 1997, **389**, 153–158.
64. R. Michener and K. Lajtha, eds. *Stable Isotopes in Ecology and Environmental Science*, 2nd edn., Blackwell, Malden, MA, 2007.
65. R. Bol, J. Marsh and T. H. E. Heaton, *Rapid Commun. Mass Spectrom.*, 2007, **21**, 2951–2954.
66. R. Bol and C. Pflieger, *Rapid Commun. Mass Spectrom.*, 2002, **16**, 2195–2200.
67. T. E. Cerling, G. Wittemyer, H. B. Rasmussen, F. Vollrath, C. E. Cerling, T. J. Robinson and I. Douglas-Hamilton, *Proc. Natl. Acad. Sci. USA*, 2006, **103**, 371–373.
68. S. Jim, S. H. Ambrose and R. P. Evershed, *Geochim. Cosmochim. Acta*, 2004, **68**, 61–72.
69. S. H. Ambrose, *J. Hum. Evol.*, 1986, **15**, 707–731.

70. T. F. Robinson, M. Sponheimer, B. L. Roeder, B. Passey, T. E. Cerling, M. D. Dearing and J. R. Ehleringer, *Small Ruminant Res.*, 2006, **64**, 162–168.
71. M. Sponheimer, T. Robinson, L. K. Ayliffe, B. H. Passey, B. Roeder, L. Shipley, E. Lopez, T. E. Cerling, D. Dearing and J. Ehleringer, *Can. J. Zool. Rev. Can. Zool.*, 2003, **81**, 871–876.
72. L. K. Ayliffe, T. E. Cerling, T. Robinson, A. G. West, M. Sponheimer, B. H. Passey, J. Hammer, B. Roeder, M. D. Dearing and J. R. Ehleringer, *Oecologia*, 2004, **139**, 11–22.
73. K. A. Hobson and R. G. Clark, *Auk*, 1993, **110**, 638–641.
74. K. A. Hobson, R. T. Alisauskas and R. G. Clark, *Condor*, 1993, **95**, 388–394.
75. M. J. DeNiro and S. Epstein, *Science*, 1977, **197**, 261–263.
76. M. J. DeNiro and S. Epstein, *Geochim. Cosmochim. Acta*, 1978, **42**, 495–506.
77. N. S. Suits, A. S. Denning, J. A. Berry, C. J. Still, J. Kaduk J. B. and Miller I. T. Baker, *Global Biogeochem. Cycles*, 2005, **19**. doi: 10.1029/2003GB002141.
78. C. J. Still, J. A. Berry G. J Collatz and R. S. DeFries, *Global Biochem. Cycles*, 2003 **17**. doi: 10.1029/2001GB01807.
79. J. W. White, K. Winters, P. Martin and A. Rossman, *J. AOAC Int.*, 1998, **81**, 610–619.
80. J. R. Brooks, N. Buchmann, S. Phillips, B. Ehleringer, R. D. Evans, M. Lott, L. A. Martinelli, W. T. Pockman, D. R. Sandquist, J. P. Sparks, L. Sperry, D. Williams and J. R. Ehleringer, *J. Agric. Food Chem.*, 2002, **50**, 6413–6418.
81. L. A. Martinelli, M. Z. Moreira, J. P. Ometto, A. R. Alcarde, L. A. Rizzon, E. Stange and J. R. Ehleringer, *J. Agric. Food Chem.*, 2003, **51**, 2625–2631.
82. L. Pissinatto, L. A. Martinelli, R. L. Victoria and P. B. de Camargo, *Food Res. Int.*, 2000, **32**, 665–668.
83. F. Besacier, R. Guilluy, J. L. Brazier, H. Chaudron-Thozet, J. Girard and A. Lamotte, *J. Forensic. Sci.* 1997, **42**, 429–433.
84. M. Desage, R. Guilluy and J. L. Brazier, *Analytica Chimica. Acta.*, 1991, **247**, 249–254.
85. F. Besacier, H. Chaudron-Thozet, M. Rousseau-Tsangaris, J. Girard and A. Lamotte, *Forensic Sci. Intl.*, 1997, **85**, 113–125.
86. J. R. Ehleringer and T. E. Cerling, *Tree Physiol.*, 1995, **15**, 105–111.
87. J. R. Ehleringer, in *Ecophysiology of Photosynthesis*, Ecological Studies Seriesed. eds. E.-D. Schulze and M. M. Caldwell, Springer, New York, 1994, pp. 361–392.
88. J. R. Ehleringer, in *Water Deficits: Plant Responses From Cell to Community*, eds. S. J. A. C. and H. Griffiths, BIOS Scientific, London, 1993, pp. 265–284.
89. J. M. Miller, R. J. WIlliams and G. D. Farquhar, *Funct. Ecol.*, 2001, **15**, 222–232.
90. J. P. Comstock and J. R. Ehleringer, *Proc. Natl. Acad. Sci. USA*, 1992, **89**, 7747–7751.
91. G. R. Stewart, M. H. Turnbull, S. Schmidt and P. D. Erskine, *Aust. J. Plant Physiol.*, 1995, **22**, 51–55.